AQUEOUS ALTERATION RINDS IN BASALT: MINERALOGIC CHARACTERIZATION FROM HAND SAMPLE TO OUTCROP WITH HYPERSPECTRAL IMAGING AND IMPLICATIONS FOR MARS 2020.

R. N. Greenberger[1], J. F. Mustard[1], E. A. Cloutis[2], P. Mann[2], and J. H. Wilson[3], [1]Dept. of Geological Sciences, Brown University, Providence, RI, 02912, Rebecca_Greenberger@brown.edu, [2]Dept. of Geography, University of Winnipeg, Winnipeg, MB, R3B 2E9, Canada. [3]Headwall Photonics, Inc., Fitchburg, MA, 01420.

Introduction: The abilities to assess context and fine-scale mineralogy remotely are important exploration goals [1]. Laboratory and field tests of these measurement capabilities can demonstrate their utility on Mars. We are performing one such test characterizing the mineralogy of hydrothermally-altered pillow basalts at thick section, hand-sample, and outcrop scales. Hydrothermally-altered deposits and hydrothermal sediments are high priority targets for future missions to Mars [1-2], and alteration rinds are important to study because the degree of water-rock interaction varies within single samples from the interior to the exterior. Rinds have been shown to be quantitatively related to these water-rock interactions [3].

Methods: Hyperspectral images were acquired of ~187 Ma hydrothermally-altered lacustrine pillow basalts in Meriden, CT [e.g., 4-6], using Channel Systems visible and near infrared imagers (0.42-1.1 µm, 10 nm spectral resolution). Images were calibrated to reflectance with a dark current subtraction and flat field correction to remove instrumental effects followed by a dark object subtraction and ratio to in-scene Spectralon® calibration target for atmospheric correction.

Laboratory images of samples and a thick section were acquired at Headwall Photonics with high efficiency visible-near infrared (VNIR; 0.4-1.0 µm, 1.785 nm spectral resolution and sampling) and shortwave infrared (SWIR; 1.0-2.5 µm, 12.0656 nm spectral resolution and sampling) imagers and were calibrated to reflectance with a dark subtraction, ratio to Spectralon®, and correction for the reflectance properties of Spectralon®. SWIR pixels were registered and scaled to corresponding VNIR pixels at 997-998 nm.

Other laboratory measurements include point spectroscopy (ASD Fieldspec 3), mineralogy (x-ray diffraction), and chemistry (inductively-coupled plasma atomic emission spectrometry [7]). The thick section was analyzed with a Cameca SX-100 electron microprobe.

Results: At all scales, the main units of altered pillow basalts (alteration rinds, interior matrix, vesicle- and fracture-fill, and material cutting through pillows) are identified with imaging spectroscopy. Spectra show increasing hydration and oxidation as hot fluids interacted with a basaltic glass protolith, though other analyses indicate that abundant glass and plagioclase remain and few clay minerals formed.

Thick section. Imaging of a thick section through the alteration rind of a pillow shows partial oxidation, hydration in the rind, calcite amygdules, and areas of calcite mixed with other phases (Fig. 1). Spectra of the interior have negative slopes suggestive of magnetite [e.g., 8-9], and there are no overtones or combination tones indicating hydration. As alteration and water-rock interaction increase from interior to exterior, a Fe^{2+}/Fe^{3+} charge transfer absorption appears in the spectra at 0.75-0.80 µm, there is a strong positive slope in the SWIR data, and an OH stretching overtone at 1.4 µm, the H-O-H combination band at 1.9 µm, and a Fe/Mg-OH combination tone near 2.31 µm strengthen [e.g., 9-10]. All of these features indicate oxidation, hydration, and recrystallization of basaltic glass with increasing alteration.

Calcite occurs in material that cuts through the pillow and as fill in vesicles and veins. It is mapped by a C-O stretching overtone at 2.34 µm and a downturn toward 2.5 µm [e.g., 11]. Imaging at this scale shows stronger 1.9 µm H-O-H combinations in calcite in the rind than the interior, indicating that exterior calcites may have higher water contents, which future work will quantify. A small area of datolite is also identified.

Microprobe analyses show that glass and albite dominate both the interior and rind of the sample with some Fe oxides also present. Na, Si, and Al in the glass and Si and possibly Al in the albite decrease in concentration from interior to exterior. In the glass, Fe, Mg, Ca, and Mn contents increase from interior to exterior. These trends are consistent with mobilization and recrystallization during alteration. The totals of the measured oxides in the glass and albite decrease from interior to exterior, probably reflecting an increase in hydration. Since no phyllosilicates were seen in this sample, the Fe/Mg-OH bonds seen with spectroscopy are likely due to this hydration within the glassy matrix.

Pillow lava cross-section. An image of a full cross-section of the altered pillow lava from which the thick section was made shows similar results (Fig. 2). While some detail is lost at the coarser spatial resolution, the larger context is more apparent in the full pillow image. The rind extends around the exterior of the pillow with strengths of the 1.4, 1.9, and 2.31 µm absorptions and the positive SWIR slope increasing from interior to exterior. These trends are apparent in a spectral transect from interior to exterior of the sample (Fig. 3). Exterior calcites also have stronger 1.9 µm features

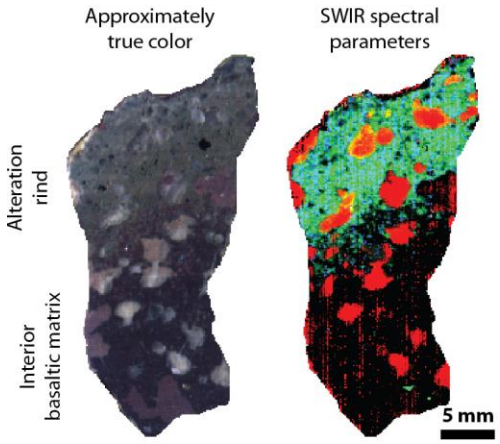

Fig. 1: Approximately true color hyperspectral image of thick section (left) and SWIR spectral parameters (right; R: Ca-rich carbonate, G: positive SWIR slope likely related to Fe^{2+}, B: Fe/Mg-rich clay).

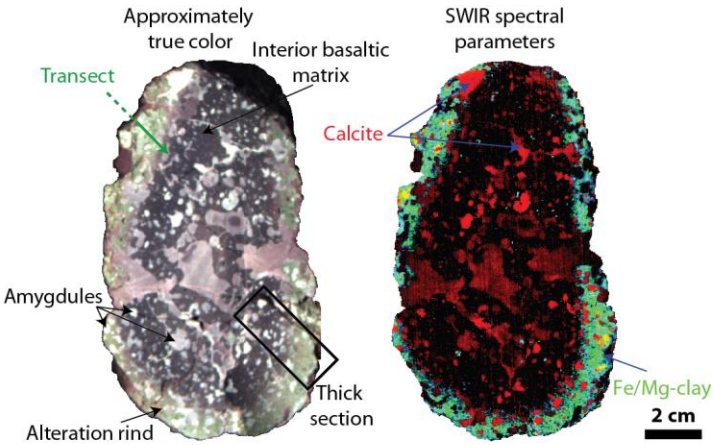

Fig. 2: Cross section of altered pillow basalt. Approximately true color hyperspectral image (left) and the same SWIR spectral parameters mapped in Fig. 1 (right).

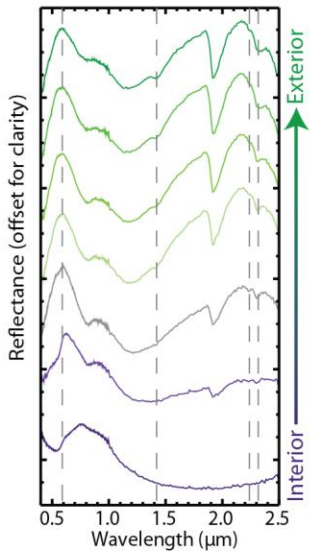

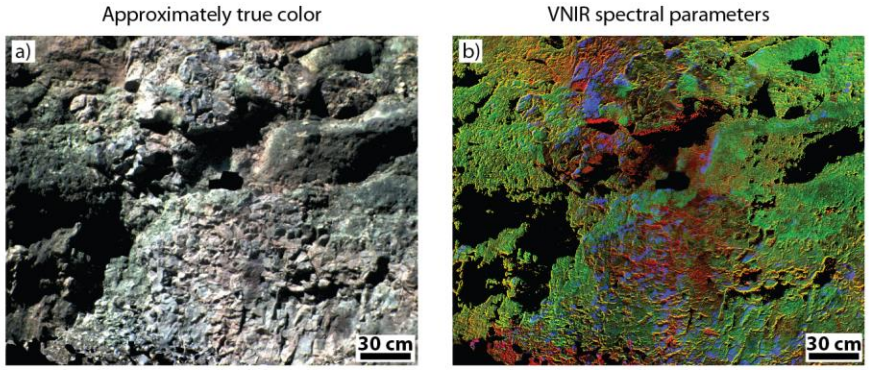

Fig. 3 (left): Spectral transect across alteration rind. Position of transect shown in Fig. 2. SWIR spectra were scaled to VNIR spectra near 1 μm.

Fig. 4 (middle and left): a) Approximately true color image outcrop. Vegetation, calibration target, and shadows have been masked. b) Visible spectral parameters (R: increase in reflectance toward red wavelengths, G: reflectance peak at green wavelengths, B: reflectance at 700 nm).

than interior ones.

Outcrop. The imagers used at the outcrop cover 0.42-1.1 μm, limiting definitive mineralogic mapping. Using laboratory data and field observations, differences in oxidation state and reflectance can be mapped and connected with mineralogies (Fig. 4). The increase in reflectance from blue to red wavelengths maps oxidation. The strength of the peak in reflectance at green wavelengths distinguishes interiors from visibly green rinds of pillows. Calcite is the brightest phases and is mapped by the reflectance at 700 nm. We would expect similar results to the laboratory with outcrop-scale imaging extending further into the infrared.

Implications for rover-scale observations on Mars: Hyperspectral imaging quickly assesses mineralogy, chemical and redox gradients, and degree of water-rock interaction at a variety of scales, from a sample the size of a thick section to a larger outcrop. These detailed mineralogic analyses would not be possible with a multispectral system such as Pancam or Mastcam [12-13]. The next steps are to incorporate chemical and XRD mapping at the thick section scale and fully encompass sample to outcrop scales as envisioned by the Mars 2020 SDT [1].

References: [1] Mustard J. F. et al. (2013), *Mars 2020 SDT Report*. [2] MEPAG E2E-iSAG (2011), *Astrobiology, 12*, 175-230. [3] Hausrath E. M. et al. (2008), *Geology, 36*, 67-70. [4] Seidemann D. E. et al. (1984) *GSA Bull., 95*, 594-598. [5] Puffer J. H. et al. (1981) *GSA Bull., 92*, 515-553. [6] Philpotts A. R. et al. (1996) *J. of Petrology, 4*, 811-836. [7] Murray R. W. et al. (2000) *ODP Tech. Note, 29*, 1-27. [8] Fischer E. M. and C. M. Pieters (1993), *Icarus, 102*, 185-202. [9] Cloutis E. A. et al. (2011), *Icarus, 212*, 180-209. [10] Clark R. N. et al. (1990), *JGR, 95*, 12653-1268. [11] Hunt G. R. and Salisbury J. W. (1971), *Modern Geol., 2*, 23-30. [12] Bell J. F. (2003), *JGR, 108*, 8063. [13] Bell J. F. (2012), *LPS XLIII*, Abstract #2541.

Acknowledgments: A. Philpotts, K. Cannon, T. Goudge, M. Peterson, and S. Wiseman for field assistance. J. Boesenberg, D. Cardace, T. Daly, D. Murray, J. Orchardo, A. Stander, K. Wilkinson, and Headwall Photonics for measurement assistance. J. Krug and Target in Meriden, CT, for allowing us to work on their property. The city of Meriden for permitting sampling.